Design of Na-CO$_2$ PCHE for Large Capacity Thermal Energy Storage System

Dehee Kim[a*], Tae-Ho Lee[a], Jonggan Hong[a], Jae-Hyuk Eoh[a]
[a]*Korea Atomic Energy Research Institute, 111 Daedeok-daero 989beon-gil, Yuseong-gu, Daejeon, Korea*
[*]*Corresponding author: dehee@kaeri.re.kr*

1. Introduction

One of fundamental limitations of renewable energy is intermittent nature of its energy source. To make up the weak points means such as thermal energy storage system (TES) can be utilized. The stored thermal energy can be converted to electricity via power conversion system stably. There are various options to store the thermal energy [1]. Representatively, an energy storage tank can take advantage of sensible heat, latent heat, and phase change heat of materials filled in the tank [1]. Number of tanks are generally one or two. One tank is favorable economically but a little complicated. System using two tanks for hot and cold tank is simple but not competitive with respect to expense.

Thermal energy storage system is connected to power conversion system for which general steam Rankine cycle can be applied or challenging supercritical CO$_2$(S-CO$_2$) Brayton cycle can be employed [2].

In this study, a conceptual design of thermal energy storage and utilization system was considered for which sensible heat storage option with two tanks and S-CO$_2$ Brayton cycle was chosen. For the storage system, sodium is used to have advantages of wide range operability of working temperature over general molten salt and high conductivity feature.

By the way, thermal energy storage system can be used to store the energy from any source including nuclear power plant.

For heat exchanger from the sodium side to the CO$_2$ side, compact printed circuit heat exchanger (PCHE) is employed [3]. To design a lumped PCHE design code had been developed [4,5] but varying properties of working fluids on temperature may require more refined design approach. Therefore, the lumped PCHE design code was upgraded to have option of discretization capability along the flow directions of both tube sides. In this study, methodology of the 1D PCHE design code is introduced in brief and the upgraded code is validated compared to the lumped code. The validated code is utilized to design Na-CO$_2$ PCHEs for thermal energy storage and utilization system based on a given plant heat balance [6].

2. Design Methods and Models

2.1 Introduction of PCHE

The Supercritical CO$_2$ Brayton cycle is not a mature technology but is getting more attention due to its promising features of high net efficiency and compact construction capability of the system. Main heat exchangers are manufactured by the type of printed circuit heat exchanger which can put up with very high operating pressure and high temperature and achieve high heat transfer rate performance. Several PCHEs are installed such as Na-CO$_2$ heat exchanger, recuperator and cooler. In this study, a simple design methodology is presented to satisfy the design requirements of the PCHE, and the preliminary design parameters are produced.

2.2 Design method of PCHE

For a PCHE design, heat transfer area, geometry of hot and cold channels are generated. Given input data are mass flow rates, temperatures and pressures of inlet and outlet and following constraints are assumed [4,5].

- semi-circular cross section of each flow channel
- straight or zig-zag flow path along the flow direction
- alternatively stacking of hot and cold plates
- ignoring heat loss to atmosphere
- manufacturing limit of 0.6 m (width) x 1.5 (length) for the PCHE plate

Governing equations are following mass, momentum and energy.

Continuity equation

$$\dot{m}_{s,total} = N_s \dot{m}_{s,ch}, \qquad (1)$$

where, $s, ch, N_s, \dot{m}_{s,total}, \dot{m}_{s,ch}$ are hot or cold side, single flow channel, total channel number of each side, total mass flow rate of each side, mass flow rate of single channel of each side, respectively.

Momentum equations

$$\Delta P_{s,total} = \sum_{i=1}^{NCV}\left(f_{s,i}\frac{\Delta L_{s,i}}{D_{h,s}} + K_{s,i}\right)\left(\frac{\dot{m}_{s,ch}}{A_{h,s,ch}}\right)^2\left(\frac{1}{2\rho_{s,i}}\right) + \left(\frac{\dot{m}_{s,ch}}{A_{h,s,ch}}\right)^2\left(\frac{1}{\rho_{s,i,out}} - \frac{1}{\rho_{s,i,in}}\right), \qquad (2)$$

where, $\Delta P_{s,total}, f, \Delta L, D_h, K, A_h, \rho, \rho_{out}, \rho_{in}$ are total pressure loss, friction loss coefficient, flow length of a control volume, hydraulic diameter of a flow channel, form loss coefficient, flow area of a flow channel, average density in a control volume, density at outlet of a control volume, density at inlet of a control volume, respectively. i, NCV are control volume index and number of control volumes along single flow channel, respectively.

Energy equation

$$Q_{s,total} = N_s \sum_{i=1}^{NCV} U_{ch,i} A_{s,ch,i} \Delta T_{LMTD,i} = N_s \sum_{i=1}^{NCV} \dot{m}_{s,ch}\left(H_{s,i,out} - H_{s,i,in}\right), \tag{3}$$

where, Q_{total}, $U, A, \Delta T_{LMTD}, H_{out}, H_{in}$ are total heat transfer rate of the heat exchanger, overall heat transfer coefficient, heat transfer area, log mean temperature difference between two sides, enthalpy at outlet of a control volume and enthalpy at inlet of a control volume, respectively.

$\dot{m}_{s,total}$, $\Delta P_{s,total}$ are given as input values and $A_{h,s,ch}, D_{h,s}, A_{s,ch}$ are calculated as follows,

$A_{h,s,ch} = \frac{\pi D_{s,ch}^2}{8}$, $D_{s,ch}$: diameter of semi-circle of single flow channel, (4)

$$D_{h,s} = \frac{4A_{h,s,ch}}{\frac{\pi D_{s,ch}}{2} + D_{s,ch}} = \frac{4A_{h,s,ch}}{P_{h,s,ch}}, \tag{5}$$

$$A_{s,ch,i} = P_{h,s,ch} \Delta L_{s,i}, \tag{6}$$

$$A_{s,total} = N_s \sum_{i=1}^{NCV} A_{s,ch,i}, \tag{7}$$

$$L_{s,total} = \sum_{i=1}^{NCV} \Delta L_{s,i}, \tag{8}$$

where, $A_{s,total}$, $L_{s,total}$ are total heat transfer area and length of single flow channel, respectively. Enthalpy, density are obtained as functions of temperature and pressure, thermal conductivity and viscosity are calculated as functions of temperature.

2.3 Configuration of channel geometry

For design, fundamental geometry information such as channel bending angle of hot channel (θ_{hot}), half length of bent channel segment (L_{seg}), pitch between cold flow channels (P_{cold}), width of single plate (Y) are given and then other geometrical information including channel bending angle of cold channel (θ_{cold}), number of bends in single hot and cold channels ($N_{bend,hot}, N_{bend,cold}$), length of single plate (X) is obtained during design process. Channel configuration is shown in Fig.1 [4].

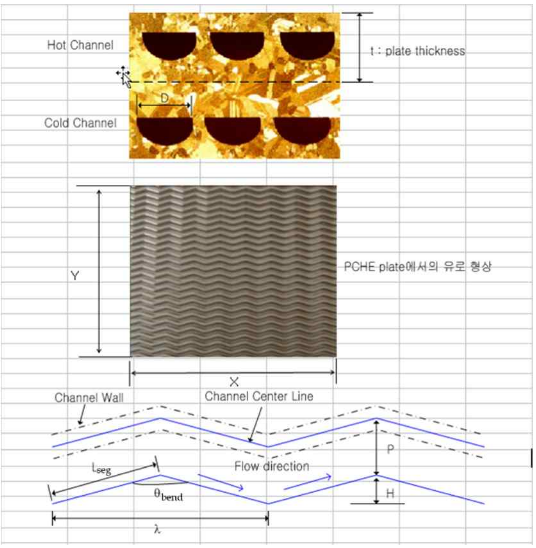

Fig. 1. Channel configuration and geometrical parameters

<u>Number of cold flow channels on single cold plate and total number of cold plates</u>

$$N_{p,cold} = \frac{Y - L_{seg,cold} \sin\left(\frac{180-\theta_{cold}}{2}\right) - D_{cold,ch}}{P_{cold}} \tag{9}$$

$$N_{ch,cold} = N_{p,cold} + 1 \tag{10}$$

$$N_{plate,cold} = \frac{N_{ch,cold,total}}{N_{ch,cold}} \tag{11}$$

where, $N_{p,cold}$, $N_{ch,cold}$, $N_{plate,cold}$, $N_{ch,cold,total}$ are number of pitches on single cold plate, number of cold flow channels on single plate, total number of cold plates and total number of cold flow channels, respectively.

<u>Number of hot flow channels on single hot plate and total number of hot plates</u>

$$N_{plate,hot} = N_{plate,cold} \tag{12}$$

$$N_{ch,hot} = \frac{N_{ch,hot,total}}{N_{plate,hot}} \tag{13}$$

$$N_{p,hot} = N_{ch,hot} - 1 \tag{14}$$

$$P_{hot} = \frac{Y - L_{seg,hot} \sin\left(\frac{180-\theta_{hot}}{2}\right) - D_{hot,ch}}{N_{p,hot}} \tag{15}$$

<u>Number of zig-zag parts for single flow channel</u>

$$N_{bend,hot} = L_{hot,total} / \left(2L_{seg,hot}\right) \tag{16}$$

$$N_{bend,cold} = L_{cold,total} / \left(2L_{seg,cold}\right) \tag{17}$$

where, $N_{bend,hot}, N_{bend,cold}$ are number of zig-zag parts for single hot and cold flow channel, respectively.

<u>Hot plate length</u>

$$X_{hot} = L_{hot,total} \cos\left(\frac{180-\theta_{hot}}{2}\right) \tag{18}$$

<u>Bending angle of cold flow channel</u>

$$X_{cold} = 2L_{seg,cold} \cos\left(\frac{180-\theta_{cold}}{2}\right) N_{bend,cold} \tag{19}$$

2.4 Correlations for heat transfer and pressure loss

Ignoring fouling factor and considering plate thickness (t), overall heat transfer coefficient is calculated as following equation.

$$U = 1/\left(\frac{1}{h_{hot}} + \frac{t}{k} + \frac{1}{h_{cold}}\right) \tag{20}$$

where, h_{hot}, k, h_{cold} are convective heat transfer coefficient of hot flow channel, conduction heat transfer coefficient through plate and convective heat transfer coefficient of cold flow channel, respectively.

Ishizuka [7] and Hesselgreaves [8] correlations can be employed.

Ishizuka correlation [7]

$$Nu = PF\frac{(f/2)(Re-1000)Pr}{1+12.7\sqrt{f/2}(Pr^{2/3}-1)} \; for \;\; Re \geq 3000 \qquad (21)$$

$$PF = 2.3, f = \frac{1}{(1.5808 \ln(Re)-3.28)^2}$$

Hesselgreaves correlation [8]

$$Nu = 4.089 \; for \;\; Re \leq 2300 \qquad (22)$$

$$Nu = 4.089 + \frac{Nu_{Re=5000} - 4.089}{5000-2300}(Re - 2300) for \;\; 2300 < Re < 5000$$

$$Nu = 0.125Re^{0.64}Pr^{0.33} \; for \;\; Re \geq 5000$$

Lockart-Martinelli correlation [9]

$$Nu = 5.0 + 0.025Re^{0.8}Pr^{0.8} \qquad (23)$$

Lockart-Martinelli correlation is used only for sodium flow.

Pressure loss is calculated by summation of frictional loss and form loss. Frictional loss coefficient can be obtained from Ishizuka model [7] and Hesselgreaves model [8].

Ishizuka model [7]

$$f = 4(0.0014 + 0.125Re^{-0.32}) \qquad (24)$$

Hesselgreaves model [8]

$$f = 11.0Re^{-0.53} \qquad (25)$$

Form loss coefficient is calculated by Idelchik [9].

$$K = N_{bend}\left(0.946\sin^2\left(\frac{180-\theta_{bend}}{2}\right) + 2.047\sin^4\left(\frac{180-\theta_{bend}}{2}\right)\right) \qquad (26)$$

Form loss effect is already included in Eq.(25) and therefore $K = 0$ for Hesselgreaves model.

2.5 Design procedure of PCHE

Flow chart of design procedure of 1D PCHE design code is displayed in Fig. 2.

3. Results

The upgraded 1D PCHE design code was validated by comparing to the lumped (0D) PCHE design code. The lumped PCHE design code had been employed to design PCHEs of ABTR, KALIMER-600 (K-600) and G4SFR [5]. The input parameters for design of the three PCHEs are summarized in Table I.

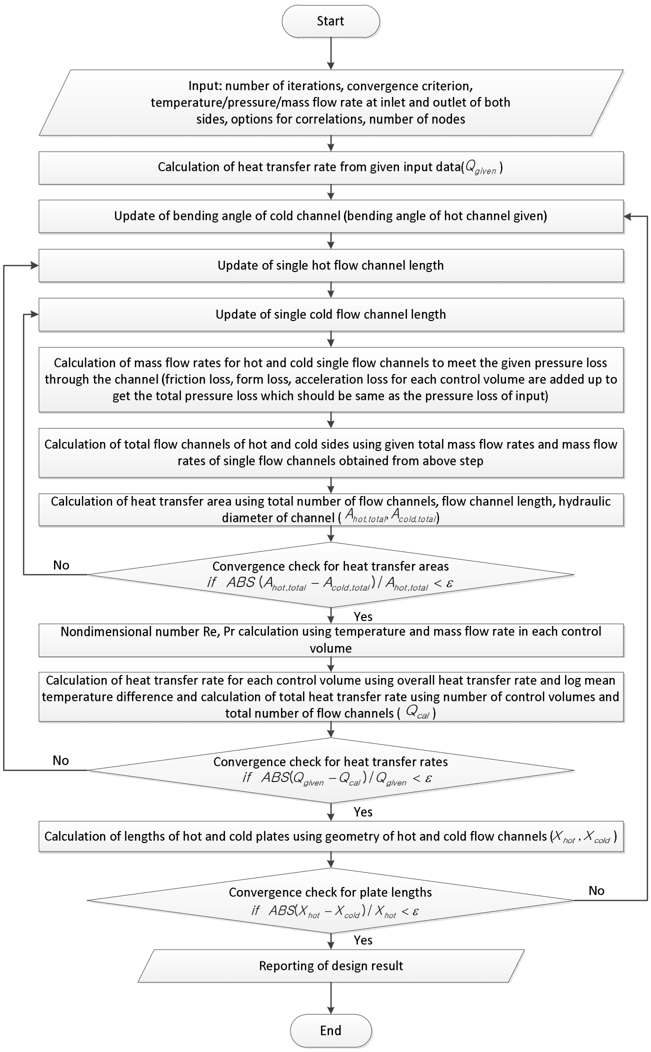

Fig. 2. Flow chart of design procedure of PCHE

Several combinations of heat transfer coefficients for hot/cold sides and pressure loss coefficients for hot/cold sides can be set up and these combinations were investigated thoroughly in [5]. Following the investigation results of best combination of correlations [5], Hesselgreaves correlation was chosen to calculate convective heat transfer coefficient for CO_2 side and Lockart-Martinelli correlation was applied for sodium side. Idelchik model was employed to calculate pressure loss.

Table II shows the designed values for the PCHEs. Differences between 0D and 1D codes are small. This indicates that for the thermo-fluid design conditions in Table I 0D design code also can be employed effectively without more detailed nodalizations of flow channels.

Table I: Design input parameters for code validation

Parameter	ABTR	K-600	G4SFR
D_{ch} [mm]	2.0	2.0	2.0
θ_{hot} [deg]	180	180	180
P_{cold} [mm]	3.0	4.0	4.0
t [mm]	2.0	2.0	2.0
L_{seg} [mm]	5.0	5.0	5.0
Y [m]	0.6	0.6	0.6
Hot channel path	Straight	Straight	Straight
Cold channel path	Zig-Zag	Zig-Zag	Zig-Zag
Hot fluid	Sodium	Sodium	Sodium
Cold fluid	CO_2	CO_2	CO_2
$T_{hot,in}$ [°C]	488.0	526.0	526.0
$T_{hot,out}$ [°C]	333.0	364.0	364.0
$T_{cold,in}$ [°C]	323.6	353.9	353.8
$T_{cold,out}$ [°C]	471.5	508.0	508.0
$P_{hot,in}$ [MPa]	0.2	0.1094	0.1094
$P_{hot,out}$ [MPa]	0.192	0.1014	0.1014
$P_{cold,in}$ [MPa]	19.91	19.94	19.94
$P_{cold,out}$ [MPa]	19.84	19.74	19.74
$\dot{m}_{hot}$ [kg/s]	19.67	7400.2	14800.4
$\dot{m}_{cold}$ [kg/s]	21.52	8076.6	16147.5

Table II: Designed data of code validation

		ABTR			K-600			G4SFR		
		0D	1D	Diff [%]	0D	1D	Diff[%]	0D	1D	Diff[%]
Heat transfer area [m^2]		129.8	130.7	0.69	42683	43121	1.03	85077	86242	1.37
N_{ch} [-]	Hot	209	208	-0.48	179	180	0.56	179	180	0.56
	Cold	199	199	0.00	149	149	0.00	149	149	0.00
Unit [m]	Length	1.17	1.17	0.00	1.05	1.04	-0.95	1.05	1.04	-0.95
	Width	0.6	0.6	0.00	0.6	0.6	0.00	0.6	0.6	0.00
	Height	0.41	0.42	2.44	176.5	178.6	1.18	352.5	357.1	1.30
θ_{cold} [deg]		145.9	145.5	-0.31	113.1	112.5	-0.53	113.1	112.5	-0.50
P_{hot} [mm]		2.875	2.885	0.34	3.349	3.338	-0.32	3.349	3.338	-0.31
$\dot{m}_{ch}$ [g/s]	Hot	0.913	0.907	-0.67	0.934	0.920	-1.49	0.935	0.920	-1.59
	Cold	1.045	1.034	-1.01	1.222	1.208	-1.17	1.223	1.207	-1.28
Q_{total} [MW]		3.906	3.892	-0.35	1529	1528	-0.02	3057	3055	-0.08

The validated code was utilized to design PCHEs in TES. Based on the system configuration and the heat balance [6], heat from sodium is transported via two Na-CO_2 PCHEs. Table III summaries input parameters for design.

Same correlations for heat transfer coefficient and pressure loss coefficient were chosen and same geometrical input parameters as K-600 and G4SFR are used for preliminary design work for TES PCHEs. Of course, these geometrical parameters and given pressure loss should be modified to reflect the features of the PCHEs in different system configuration and to be able to get more optimal design.

Table III: Design input parameters for TES PCHEs

Parameter	PCHE1	PCHE2
D_{ch} [mm]	2.0	2.0
θ_{hot} [deg]	180	180
P_{cold} [mm]	4.0	4.0
t [mm]	2.0	2.0
L_{seg} [mm]	5.0	5.0
Y [m]	0.6	0.6
Hot channel path	Straight	Straight
Cold channel path	Zig-Zag	Zig-Zag
Hot fluid	Sodium	Sodium
Cold fluid	CO_2	CO_2
$T_{hot,in}$ [°C]	700.0	380.0
$T_{hot,out}$ [°C]	380.0	200.0
$T_{cold,in}$ [°C]	360.4	114.1
$T_{cold,out}$ [°C]	515.0	360.4
$P_{hot,in}$ [MPa]	0.1174	0.1094
$P_{hot,out}$ [MPa]	0.1094	0.1014
$P_{cold,in}$ [MPa]	28.53	28.73
$P_{cold,out}$ [MPa]	28.33	28.53
$\dot{m}_{hot}$ [kg/s]	156.02	156.02
$\dot{m}_{cold}$ [kg/s]	323.70	98.73

Table IV: Designed data of TES PCHEs

		PCHE1			PCHE2		
		0D	1D	Diff[%]	0D	1D	Diff[%]
Heat transfer area [m^2]		206.9	208.8	0.92	271.7	278.6	2.54
N_{ch} [-]	Hot	159	159	0.00	272	250	-8.09
	Cold	150	150	0.00	149	149	0.00
$N_{ch,total}$ [-]	Hot	103710	103434	-0.27	115243	114413	-0.72
	Cold	97369	97523	0.16	63183	68266	8.04
L_{total} [mm]	Hot	388.07	392.58	1.16	458.59	473.63	3.28
	Cold	413.34	419.32	1.45	836.45	793.71	-5.11
Unit [m]	Length	0.39	0.39	0.00	0.46	0.47	2.17
	Width	0.6	0.6	0.00	0.6	0.6	0.00
	Height	2.60	2.60	0.00	1.69	1.83	8.28
θ_{cold} [deg]		139.72	139.04	-0.49	66.50	73.30	10.23
P_{hot} [mm]		3.7647	3.7810	0.43	2.2018	2.3960	8.82
$\dot{m}_{ch}$[g/s]	Hot	1.5044	1.5084	0.27	1.3538	1.3637	0.73
	Cold	3.3245	3.3192	-0.16	1.5626	1.4462	-7.45
Q_{total} [MW]		63.1905	62.9285	-0.41	36.2439	36.8457	1.66

Designed data are shown in Table IV. For PCHE1 design, 0D design code and 1D design code are similar but for PCHE2 design, two codes made meaningful differences. The reason of different results can be deduced by comparing the overall heat transfer coefficient. For PCHE1, along the nodes (or control volume) overall heat transfer coefficient vary monotonously but for PCHE2 the variation profile of overall heat transfer coefficient is not linear. Therefore, 0D approach which can be considered as averaging method of values of two ends may not be enough to reflect the local heat transfer feature accurately.

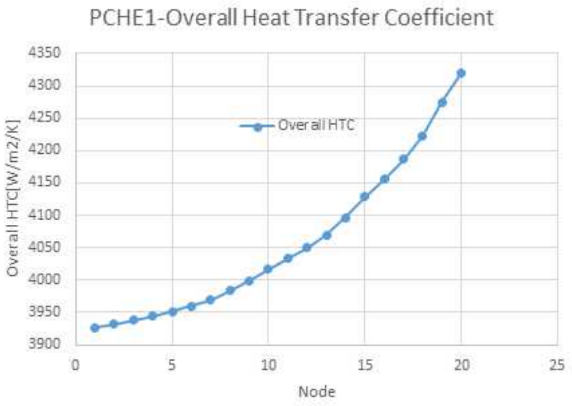

Fig. 3. Overall heat transfer coefficients of PCHE1

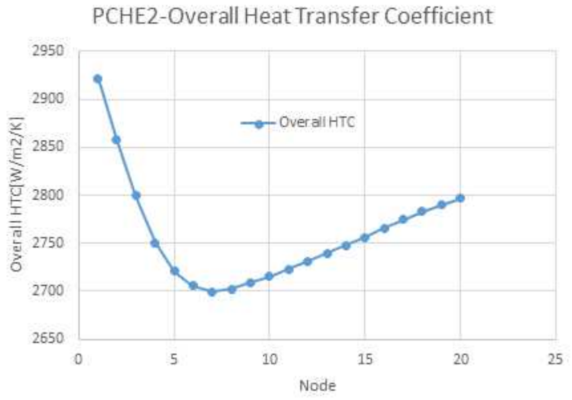

Fig. 4. Overall heat transfer coefficients of PCHE2

4. Conclusion

A lumped PCHE design code was upgraded to 1D design code to reflect 1D local effect along the flow direction. The upgraded code was validated through several PCHE designs for SFRs. Finally, the code was employed to design PCHEs installed for thermal energy storage and utilization system. Partial heating configuration of the system is equipped with two PCHEs to transfer heat from sodium to CO_2. For some cases, overall heat transfer coefficient along the nodes varies in a nonlinear pattern. For this case, 0D design approach may not fully reflect the local heat transfer features of PCHE and for this case 1D design approach can be a more proper tool for PCHE design.

ACKNOWLEDGEMENT

This work was supported by the National Research Council of Science & Technology (NST) grant funded by the Korean government (MSIT) [No. CAP-20-03-KAERI].

REFERENCES

[1] N. Niedermeier, J. Flesch, L. Marocco and Th. Wetzel, Assessment of Thermal Energy Storage Options in a Sodium-based CSP Plant, Applied Thermal Engineering, Vol.107, pp.386-397, 2016.
[2] K. Gezelius, M.J. Driscoll and P. Hejzlar, Design of Compact Intermediate Heat Exchanger for Gas Cooled Fast Reactor, MIT-ANP-TR-103, MIT, 2004.
[3] Heatric^{TM}, hppt://www.heatric.com/.
[4] T.H. Lee, J.E. Cha, J.H. Eoh, S.O. Kim and D.H. Hahn, Preliminary Design of PCHE in S-CO_2 Brayton Cycle Coupled to KALIMER-600, KNS Spring Meeting, 2008.
[5] T.H. Lee, Report of Heat Balance Calculation of G4SFR and KALIMER-600 with Supercritical CO_2 Brayton Cycle and PCHE Design, LMR/FS400-AR-01Rev.0/07, KAERI, 2007.
[6] S.R. Choi, Heat Balance Calculation for Large-capacity Thermal Energy Storage and Utilization System, CAP/TS310-CA-01/2020, KAERI, 2021.
[7] T. Ishizuka et al., Thermal-Hydraulic Characteristics of a Printed Circuit Heat Exchanger in a Supercritical CO_2 Loop, Proceedings of 11th Int. Topical Conf. on Nuclear Reactor Thermal-Hydraulics, Avignon, France, Oct. 2-6, 2005.
[8] J.E. Hesselgreaves, Compact Heat Exchangers, Selection, Design and operation, 1st edition, Pergamon, 2001.
[9] N.E. Todreas and M.S. Kazimi, Nuclear Systems I-Thermal Hydraulic Fundamentals, Hemisphere Publishing Co., 1990.
[10] I.E. Idelchik, Handbook of Hydraulic Resistance, 2nd edition, Hemisphere Publishing Co., 1986.